

# Increased Arctic cloud longwave emissivity associated with pollution from mid-latitudes

Timothy J. Garrett<sup>1</sup> & Chuanfeng Zhao<sup>1</sup>

There is consensus among climate models that Arctic climate is particularly sensitive to anthropogenic greenhouse gases and that, over the next century, Arctic surface temperatures are projected to rise at a rate about twice the global mean<sup>1</sup>. The response of Arctic surface temperatures to greenhouse gas thermal emission is modified by Northern Hemisphere synoptic meteorology and local radiative processes<sup>2–4</sup>. Aerosols may play a contributing factor through changes to cloud radiative properties. Here we evaluate a previously suggested contribution of anthropogenic aerosols to cloud emission and surface temperatures in the Arctic<sup>5–8</sup>. Using four years of ground-based aerosol and radiation measurements obtained near Barrow, Alaska, we show that, where thin water clouds and pollution are coincident, there is an increase in cloud longwave emissivity resulting from elevated haze levels. This results in an estimated surface warming under cloudy skies of between 3.3 and 5.2 W m<sup>-2</sup> or 1 and 1.6 °C. Arctic climate is closely tied to cloud longwave emission<sup>2,4,9</sup>, but feedback mechanisms in the system are complex<sup>10</sup> and the actual climate response to the described sensitivity remains to be evaluated.

Previous studies of the effects of anthropogenic aerosols on cloud radiative properties have emphasized their potential contributions to planetary cooling, through greater activation of cloud droplets, and an accompanying increase in the reflection to space of solar energy<sup>1,11,12</sup>. Large, soluble aerosols act as cloud condensation nuclei (CCN). In what is known as the ‘first indirect effect’<sup>11</sup>, for a fixed water path  $W$ , pollution increases shortwave (SW) cloud albedo  $\alpha$  because higher concentrations of CCN correspond to smaller droplets with higher number concentrations  $N$ , and hence higher cloud scattering cross-sections. This sensitivity can be quantified through  $S_{SW} = (d\alpha/dN)_W$ . In pristine stratus clouds,  $S_{SW}$  might range as high as 0.01 cm<sup>3</sup>, sufficient to partly offset greenhouse gas warming<sup>1,12</sup>.

Our goal here to is evaluate a hypothesized contribution to cloud longwave (LW) emission and surface temperatures from the long-range transport to the Arctic of mid-latitude anthropogenic aerosols<sup>5–7</sup>. Cloud thermal emission follows the relation  $F_{LW} = \varepsilon\sigma_{SB}T^4$ , where  $\varepsilon$  is the emissivity,  $\sigma_{SB}$  the Stefan–Boltzmann constant and  $T$  temperature. Emissivity is related to cloud properties through  $\varepsilon = 1 - \exp(-kW)$ , where  $W = 4/3\pi\rho r^3Nh$  ( $\rho$  being the bulk density of water,  $r$  the mean droplet radius, and  $h$  the cloud thickness), and  $k$  depends on the wavelength and cloud droplet size. Traditionally, the relationship between CCN concentrations and  $\varepsilon$  has not been a focus, because it has often been assumed that values of  $W$  in water clouds are greater than about 50 g m<sup>-2</sup>, in which case they approximate a blackbody ( $\varepsilon \approx 1$ ); accordingly,  $\varepsilon$  is insensitive to changes in cloud microstructures. However, in recent years, better detection techniques have increased awareness of thin water clouds<sup>13</sup>. As greybodies, with  $\varepsilon < 1$ , it is hypothesized that the emissivity of these clouds may be linked to changes in droplet concentration<sup>7</sup>. From estimates of  $k$  (ref. 7), it is straightforward to show that the LW sensitivity of  $\varepsilon$  to  $N$ ,  $S_{LW} = (d\varepsilon/dN)_W$  is given by Fig. 1.

$S_{LW}$  exceeds 0.01 cm<sup>3</sup> in pristine clouds with  $N < 10$  cm<sup>-3</sup> and  $W < 25$  g m<sup>-2</sup>.

In the Arctic, this LW indirect effect is relevant because the surface radiation balance between winter and early spring is tied to downwelling thermal fluxes from thin, greybody, low to mid-level clouds<sup>14,15</sup>. At this time of year, the Arctic is characterized by widespread pollution known as Arctic haze. Strong east–west pressure gradients cause episodic northward intrusions of polluted air from mid-latitude Eurasia and North America<sup>16,17</sup>. Because precipitation is low, aerosol lifetimes are long<sup>18</sup>, and pollution accumulates through the depth of the lower troposphere<sup>19</sup>. Arctic haze only disperses when moist destabilizing air intrudes in spring<sup>20</sup>. Indirect solar forcing by the haze aerosol is usually small or negligible because the polluted months are either dark, or characterized by high solar zenith angles and a surface that is already bright<sup>14,15</sup>. Instead, clouds are thin, so there is significant potential for increased surface warming from aerosol modifications to cloud LW emissivity<sup>7</sup>.

To examine this more closely, we use long-term ground-based data sets from two adjacent sites near Barrow, Alaska, supervised by the DOE Atmospheric Radiation Measurement (ARM) programme<sup>21</sup>,

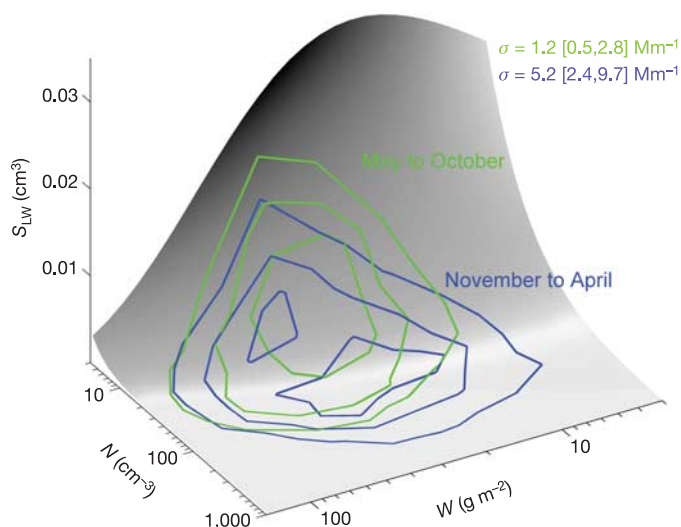


**Figure 1 | Sensitivity of cloud LW emissivity to changes in droplet number concentration for fixed water path,  $S_{LW} = (d\varepsilon/dN)_W$ .** The surface is theoretically based, assuming a cloud depth and temperature of 100 m and 253 K, respectively. Superimposed contours show quartiles in distributions of ground-based retrievals<sup>27</sup> of low-level water cloud number concentration  $N$  and liquid water path  $W$  from near Barrow, Alaska, between 2000 and 2003. Relative pollution levels for the contours are indicated by mean values of  $\sigma$  with [lower, upper] quartiles ( $\sigma$  is the 550 nm light scattering cross-section density of effloresced aerosol particles).

<sup>1</sup>Department of Meteorology, University of Utah, Salt Lake City, Utah 84112, USA.

and by the NOAA Climate Monitoring Diagnostics Laboratory (CMDL)<sup>22</sup>. No measurements were made of CCN at either site. Instead, relative pollution levels are inferred from CMDL measurements of  $\sigma$ , the 550 nm light scattering cross-section density of effloresced aerosol particles. Usually CCN and  $\sigma$  correlate closely<sup>23,24</sup> because the size range of aerosol normally associated with CCN is also highly efficient at scattering light. Measurements are limited to particles smaller than 1  $\mu\text{m}$ . This is done to exclude natural contributions from larger Asian dust aerosol, which can initiate a conversion to ice in super-cooled water clouds<sup>25</sup>. Analyses are further limited to time periods when the CMDL was upwind of Barrow. Retrievals of cloud  $\varepsilon$ ,  $W$ ,  $r_e$  (the area-weighted mean—or effective—radius of the droplet size distribution) and  $N$  are obtained using a ground-based Fourier transform infrared spectrometer (FTIR), lidar, radar, and temperature and humidity soundings from ARM, together with Global Ozone Monitoring Experiment (GOME) stratospheric ozone profiles from aboard the European Space Agency's Second European Remote Sensing Satellite (ERS-2)<sup>26</sup>. The retrieval method is based on one developed previously for application to ice clouds in the Antarctic<sup>27</sup>. To reduce uncertainty associated with vertical stratification when comparing surface aerosol measurements to retrieved cloud properties<sup>19</sup>, we restrict analyses to single-layer clouds with tops below 1.5 km altitude. Following application of the above restrictions, 9,440 5-min cloud samples were examined for the years between 2000 and 2003.

During this period, median retrieved droplet concentrations in greybody Arctic stratus were higher between November and April (56  $\text{cm}^{-3}$ , 3,040 samples) than in the less polluted May to October (27  $\text{cm}^{-3}$ , 6,400 samples) (Fig. 1). The late spring to autumn values are consistent with *in situ* measurements from the pristine central Arctic in summer<sup>28</sup>. We then estimate from Fig. 1 that the LW sensitivity of clean Arctic stratus to changes in CCN concentration is  $S_{LW} = 0.002 \text{ cm}^3$ . We may assess the potential for cloud emissivity perturbation due to long-range transport of pollution as follows: clouds important to the Arctic LW surface radiation balance have bases typically below about 4 km altitude<sup>15</sup>. To raise concentrations of typical haze aerosol that might act as CCN<sup>16</sup> to this depth by 1  $\text{cm}^{-3}$  over the entire Arctic requires about 1 kt of material. The characteristic lifetime of Arctic haze particles ranges up to 39 days (ref. 18). Accordingly, sustaining a uniform anthropogenic increase in CCN concentrations of about 5  $\text{cm}^{-3}$  (the amount necessary for a nominal increase to  $\varepsilon$  of  $\sim 0.01$ ) requires long range transport to the Arctic of between 10 and 100 kt of material per year. For comparison, this is just 1% of the 1–10 Mt  $\text{yr}^{-1}$  anthropogenic  $\text{SO}_2$  made available to the Arctic from the Eurasian region north of 60° latitude alone<sup>16</sup>. Therefore, mid-latitude pollution should be sufficient to alter Arctic cloud LW properties.

The sensitivity of low-level cloud emissivity to pollution near Barrow is shown in Fig. 2a. Retrievals of cloud  $\varepsilon$  are sorted according to upper (polluted) and lower (clean) quartile thresholds in  $\sigma$ . To isolate the sensitivity to  $N$  when  $\varepsilon$  is also sensitive to  $W$ , values of  $\varepsilon$  are grouped into four logarithmically spaced bins in  $W$ , according to the exponential relationship between  $\varepsilon$  and  $W$ . As an artefact of the binning, there are small differences in mean  $W$  that bias differences in the mean values of  $\varepsilon$  for each cohort, but by at most +0.01. As expected,  $\varepsilon$  is insensitive to pollution in clouds with  $W > 40 \text{ g m}^{-2}$ , because the clouds already approximate blackbodies. In thinner clouds, however, a one-sided Student  $t$ -test shows, to within 95% confidence ( $t > 4.0$  in each case), that polluted clouds have higher average values of  $\varepsilon$  than clean clouds with similar mean  $W$ :  $\Delta\varepsilon$  ranges from 0.05 for the 5–10  $\text{g m}^{-2}$  bin, to 0.08 for the 20–40  $\text{g m}^{-2}$  bin. The reason that higher values of greybody emissivity occurred in the nominally polluted clouds was that their droplets had, on average, values of  $r_e$  that were 3  $\mu\text{m}$  smaller, and concentrations three times more numerous, than droplets in nominally clean clouds.

Measurements from the SHEBA (Surface Heat Budget of the Arctic) experiment show that LW surface radiative forcing  $\text{CF}_{LW}$  by blackbody

clouds is  $65 \pm 10 \text{ W m}^{-2}$  (ref. 15). Long-term measurements from drifting ice stations show that, between November and March, cloudy sky  $\text{CF}_{LW}$  is between 20 and 30  $\text{W m}^{-2}$  and that, following a winter-time transition from clear to cloudy skies, Arctic surface temperatures increase by 6 to 9 K over 1 to 2 days (ref. 14). From these observations, and the results shown in Fig. 2a, we estimate that the upper quartile in  $\sigma$  is associated with an average additional 3.3–5.2  $\text{W m}^{-2}$ , or 1 to 1.6 K surface warming by clouds, compared to the lower quartile in  $\sigma$ . Such sensitivity is consistent with previous estimates<sup>24</sup>, based on more theoretical considerations, which predicted that a doubling in  $\sigma$  would increase Arctic  $\text{CF}_{LW}$  by 2  $\text{W m}^{-2}$ . More recently, pyrgeometer data were used to attribute an average 8.2  $\text{W m}^{-2}$  increased surface LW flux to aerosols from industrial emissions, 3.4  $\text{W m}^{-2}$  of which was from changes to cloud  $r_e$  alone<sup>8</sup>.

An added consideration to our analysis is that, to be important to the Arctic surface radiation balance, clouds and pollution must coincide. Near Barrow, pollution levels are in the upper quartile of the entire data set at least one-half of the time between December and March (Fig. 2b). During this period, single-layer liquid clouds with bases below 4 km are normally greybodies. Their coverage,  $A$ , is less than in summer, but is nonetheless nearly one-half. It is difficult to compare simultaneous measurements of  $\sigma$  at the ground with cloud properties well aloft. However, our data set showed that high pollution levels were present 60% of the time when low-level water clouds with tops <1.5 km were present. More representative of the Arctic as a whole, ice station data show that  $A$  varies between 0.5 and 0.6 in winter<sup>14</sup>, slightly more often than near Barrow.

We note that smaller additional LW aerosol forcing might be expected from pollution events in the two middle quartiles of  $\sigma$ . Further, it is possible that LW aerosol forcing may be modified by feedbacks that increase or decrease cloudy thermal emission through changes to cloud  $W$  and  $A$ . During the darker months, Arctic stratus

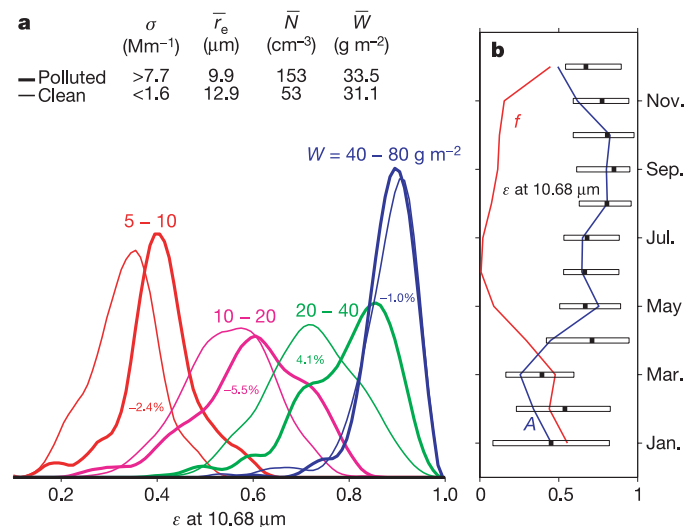


**Figure 2 | Surface-based observations of Arctic pollution, clouds, and their radiative properties, made near Barrow, Alaska.** **a**, Restricting cloud tops to below 1.5 km, we show probability distribution functions of values of liquid cloud emissivity  $\varepsilon$  within an atmospheric window at 10.68  $\mu\text{m}$  wavelength. Values are sorted according to the upper (polluted) and lower (clean) quartile thresholds in surface measurements of  $\sigma$ , and binned according to retrieved values of water path,  $W$ . Differences in mean  $W$  between each pollution cohort are shown in per cent. Mean cloud properties shown are for greybody clouds only ( $r_e$ , area-weighted effective radius of the droplet size distribution;  $N$ , number concentration of droplets). **b**, For single-layer liquid clouds with bases less than 4 km (those radiatively important to the surface LW balance<sup>15</sup> and for which cloud properties could be retrieved), we show the monthly-averaged cycle in  $\varepsilon$  (shown as a quartile plot), cloud coverage  $A$ , and the fraction of time  $f$  that  $\sigma$  is in the upper quartile for the entire data set.

is largely decoupled from the surface, and it maintains itself through cloud-top thermal emission<sup>29</sup>. Although aerosol–cloud emissivity feedbacks are poorly understood, they are likely to be positive in this case because cloud-top thermal emission is proportional to  $\epsilon$ . Airborne observations of a transition from clean to polluted air in a summer Arctic stratus deck showed increasing  $N$  and decreasing  $r_e$ , but also a halt to precipitation, higher water contents, and higher cloud  $A$  (ref. 7).

## METHODS

Greybody cloud  $r_e$  and  $W$  are inferred using a minimization technique so that they are theoretically consistent with (1) FTIR retrievals of cloud  $\epsilon$ , centred at two frequencies (862.5 and 935.8  $\text{cm}^{-1}$ ) in the atmospheric window where gaseous emission is particularly small, and (2) cloud transmission of stratospheric ozone emission centred at 1,040  $\text{cm}^{-1}$  (ref. 27). This method is particularly well suited to high latitudes, because clouds tend to be greybodies, continuum emission by water vapour is low, and equilibrium stratospheric ozone concentrations are high. We have made several minor modifications to this technique. Instead of  $\text{CO}_2$  slicing, we use lidar, radar, and ARM atmospheric soundings to determine cloud base, top, and temperature and humidity profiles, respectively. Second, water rather than ice clouds are selected<sup>30</sup> because, at low levels, super-cooled water clouds predominate in the Arctic, even at temperatures well below freezing<sup>10</sup>. Errors in retrievals for greybody clouds with  $W < 40 \text{ g m}^{-2}$  were estimated from comparisons with the retrieved properties of synthetic plane-parallel clouds, and from the model sensitivities to uncertainties in the measurements. Combined, estimated errors are to within 10% for  $r_e$ ,  $W$  and  $\epsilon$ , and 30% for  $N$ . Cloud droplet number concentration is related to  $r_e$  and  $W$  by  $N = 3W \exp(3s^2)/4\pi r_e^3 h$ , where  $s$  is an assumed width of a log-normal droplet size distribution (a value of  $0.32 \pm 0.1$  is chosen here on the basis of aircraft measurements)<sup>24</sup>.

Received 29 July 2005; accepted 3 February 2006.

- Houghton, J. T. *et al.* (eds) *Climate Change 2001: The Scientific Basis* (Cambridge Univ. Press, Cambridge, UK, 2001).
- Overland, J. E., Adams, J. M. & Bond, N. A. Regional variation of winter temperatures in the Arctic. *J. Clim.* **10**, 821–837 (1997).
- Wang, X. & Key, J. R. Recent trends in Arctic surface, cloud, and radiation properties from space. *Science* **299**, 1725–1728 (2003).
- Vavrus, S. The impact of cloud feedbacks on Arctic climate under greenhouse forcing. *J. Clim.* **17**, 603–615 (2004).
- Zhang, T., Stamnes, K. & Bowling, S. A. Impact of clouds on surface radiative fluxes and snowmelt in the Arctic and subarctic. *J. Clim.* **9**, 2110–2123 (1996).
- Curry, J. & Ebert, E. Sensitivity of the thickness of Arctic sea ice to the optical properties of clouds. *Ann. Glaciol.* **14**, 43–46 (1990).
- Garrett, T. J., Radke, L. F. & Hobbs, P. V. Aerosol effects on the cloud emissivity and surface longwave heating in the arctic. *J. Atmos. Sci.* **59**, 769–778 (2002).
- Lubin, D. & Vogelmann, A. M. A climatologically significant aerosol longwave indirect effect in the Arctic. *Nature* **439**, 453–456 (2006).
- Miller, J. R. & Russell, G. L. Projected impact of climate change on the energy budget of the Arctic Ocean by a global climate model. *J. Clim.* **15**, 3028–3042 (2002).
- Curry, J. A., Rossow, W. B., Randall, D. & Schramm, J. L. Overview of Arctic cloud and radiation characteristics. *J. Clim.* **9**, 1731–1764 (1996).
- Twomey, S. The influence of pollution on the shortwave albedo of clouds. *J. Atmos. Sci.* **34**, 1149–1152 (1977).
- Twomey, S. Aerosol, clouds, and radiation. *Atmos. Environ. A* **25**, 2435–2442 (1991).
- Marchand, R. *et al.* An assessment of microwave absorption models and retrievals of cloud liquid water using clear-sky data. *J. Geophys. Res.* **108**, 4773, doi:10.1029/2003JD003843 (2003).
- Walsh, J. E. & Chapman, W. L. Arctic cloud-radiation-temperature associations in observational data and atmospheric reanalyses. *J. Clim.* **11**, 3030–3045 (1998).
- Shupe, M. D. & Intrieri, J. M. Cloud radiative forcing of the Arctic surface: the influence of cloud properties, surface albedo, and solar zenith angle. *J. Clim.* **17**, 616–628 (2004).
- Barrie, L. A. Arctic air pollution: an overview of current knowledge. *Atmos. Environ.* **20**, 643–663 (1986).
- Polissar, A. V. *et al.* The aerosol at Barrow, Alaska: long-term trends and source locations. *Atmos. Environ.* **33**, 2441–2458 (1999).
- Baskaran, M. & Shaw, G. E. Residence time of arctic haze aerosols using the concentrations and activity ratios of <sup>210</sup>Po, <sup>210</sup>Pb and <sup>7</sup>Be. *J. Aerosol. Sci.* **32**, 443–452 (2001).
- Wylie, D. P. & Hudson, J. G. Effects of long-range transport and clouds on cloud condensation nuclei in the springtime Arctic. *J. Geophys. Res.* **107**, doi:10.1029/2001JD000759 (2002).
- Sirois, A. & Barrie, L. A. Arctic lower tropospheric aerosol trends and composition at Alert, Canada: 1980–1995. *J. Geophys. Res.* **104**, 11599–11618 (1999).
- Stamnes, K., Ellingson, R. G., Curry, J. A., Walsh, J. E. & Zak, B. D. Review of science issues, deployment strategy, and status for the ARM North Slope of Alaska-Adjacent Arctic Ocean climate research site. *J. Clim.* **12**, 46–63 (1999).
- NOAA CMDL Point Barrow Observatory. (<http://www.cmdl.noaa.gov/obop/BRW/>) (2005).
- Radke, L. F., Hobbs, P. V. & Pinnons, J. E. Observations of cloud condensation nuclei, sodium-containing particles, ice nuclei and the light-scattering coefficient near Barrow, Alaska. *J. Appl. Meteorol.* **15**, 982–995 (1976).
- Garrett, T. J., Zhao, C., Dong, X., Mace, G. G. & Hobbs, P. V. Effects of varying aerosol regimes on low-level Arctic stratus. *Geophys. Res. Lett.* **31**, doi:10.1029/2004GL019928 (2004).
- Sassen, K. Dusty ice clouds over Alaska. *Nature* **434**, 456 (2005).
- Burrows, J. P. *et al.* The Global Ozone Monitoring Experiment GOME: Mission concept and first scientific results. *J. Atmos. Sci.* **56**, 151–175 (1999).
- Mahesh, A., Walden, V. P. & Warren, S. G. Ground-based remote sensing of cloud properties over the Antarctic Plateau. Part II: Cloud optical depths and sizes. *J. Appl. Meteorol.* **40**, 1279–1294 (2001).
- Bigg, E. K. & Leck, C. Cloud-active particles over the central Arctic Ocean. *J. Geophys. Res.* **106**, 32155–32166 (2001).
- Morrison, H. & Pinto, J. O. Mesoscale modeling of springtime Arctic mixed-phase stratiform clouds using a new two-moment bulk microphysics scheme. *J. Atmos. Sci.* **62**, 3683–3704 (2005).
- King, M. D. *et al.* Remote sensing of liquid water and ice cloud optical thickness and effective radius in the Arctic: Application of airborne multispectral MAS data. *J. Atmos. Ocean. Technol.* **21**, 857–875 (2004).

**Acknowledgements** This work was supported by the National Science Foundation. J. Ogren provided CMDL data. V. Walden and A. Mahesh provided assistance with retrieval development.

**Author Contributions** Both authors contributed equally to this manuscript.

**Author Information** Reprints and permissions information is available at [npg.nature.com/reprintsandpermissions](http://npg.nature.com/reprintsandpermissions). The authors declare no competing financial interests. Correspondence and requests for materials should be addressed to T.J.G. ([tgarett@met.utah.edu](mailto:tgarett@met.utah.edu)).